S/X-Band Experiment: A Study of the Effects of Multipath on Group Delay

T. Y. Otoshi
Communications Elements Research Section

An analytical expression is presented for calculating the effects of multipath on group delay. The expression was experimentally verified by tests made at the Telecommunications Development Laboratory using the Mariner Venus/Mercury 1973 Radio Frequency Subsystem, Block 3 receiver and the Mu 1 ranging machine.

I. Introduction

With the exception of DSS 14, all stations of the Deep Space Network use the conventional zero-delay ranging configuration, in which the zero-delay device (ZDD) is mounted on the dish surface. A zenith range measurement via the airpath to a dish-mounted ZDD and a Z-height correction (Ref. 1) provide needed ground station information for determining the true range to the spacecraft.

Results of airpath tests at DSS 14 showed that large changes in range occurred as a function of antenna elevation angle when a ZDD was mounted on the 64-m antenna dish surface (Ref. 2). This characteristic was also observed on the 64-m antenna systems at DSS 43 and DSS 63 (Ref. 3). Since the range dependence on elevation angle could be due to a multipath phenomenon, one cannot assume that a zenith measured value is the correct value.

Other airpath tests made on the 64-m antenna S/X system at DSS 14 showed that large-range changes also occurred when small changes were made in axial focusing of the hyperbola. Another unexplained airpath phenomenon observed was a 53-ns discrepancy between the theoretical and experimental values of S-band zero delay range when the dichroic plate/ellipsoid assembly was retracted and the system was operated for S-band only (Ref. 4). Because of the described airpath problems, the ZDD configuration at DSS 14 has been operated in a cable configuration (Ref. 5) since January 12, 1974.

Although it had been suspected that some of the airpath problems could be due to multipath, other system testing priorities made it difficult to perform further airpath tests to isolate the source of the problems. It was also thought that multipath could not generate errors of the magnitudes which were observed. Recently, the study of the multipath effect was reinitiated and resulted in the

derivations of two theoretical expressions which showed that surprisingly large errors on range measurements could be caused by multipath. One expression derived by J. R. Smith (Refs. 6, 7) is based on the phase shift produced on the envelope of a carrier that is phase-modulated with a square-wave. The analysis was done for the range-clock modulation and detection processes actually employed by the Planetary and Mu-Ranging systems. The second expression, which was derived independently by this author, is based on the conventional definition of group delay where the output phase of a carrier wave is differentiated with respect to frequency. It was shown by Smith (Ref. 7) that for low range-clock modulation frequencies, the two independent derivations reduced to the same mathematical expression.

This article presents the theoretical expression derived by this author and the test data obtained at the Telecommunications Development Laboratory (TDL), showing good agreement between theory and experiment.

II. Summary of Theoretical Expressions

Figure 1 shows the multipath configuration for which the theory was derived. Path 1 is the primary path, and path 2 is the leakage path. The group delay (in seconds) for a signal to travel from the input port to the output port can be expressed as

$$t_g = t_{g1} + \epsilon_g \tag{1}$$

where t_{g1} is the group delay which would be observed in the absence of multipath, and ϵ_g is the deviation from t_{g1} caused by multipath. As derived in the Appendix, this error term is given by

$$\epsilon_g = A(t_{g2} - t_{g1})\left[\frac{A + \cos\theta}{1 + 2A\cos\theta + A^2}\right] \tag{2}$$

where

$$\theta = -(\beta_2 \ell_2 - \beta_1 \ell_1) \tag{3}$$

and where

A = ratio of the magnitude of the leakage wave to the magnitude of the primary wave

β_1, β_2 = phase constants, respectively, of paths 1 and 2, rad/m

ℓ_1, ℓ_2 = physical path lengths, respectively, of paths 1 and 2, m

t_{g1} = group delay of the primary wave traveling through path 1 only, s

t_{g2} = group delay of the leakage wave traveling through path 2 only, s

It is also shown in the Appendix that the carrier phase delay in seconds is

$$t_p = t_{p1} + \epsilon_p \tag{4}$$

where

$$\epsilon_p = -\frac{1}{\omega}\tan^{-1}\left[\frac{A\sin\theta}{1 + A\cos\theta}\right] \tag{5}$$

The differenced range versus integrated doppler (DRVID) can be calculated from (See Ref. 8)

$$\text{DRVID} = t_g - t_p \tag{6}$$

and relative carrier amplitude in dB from

$$20\log_{10}\left|\frac{E_{\text{out}}}{E_{\text{in}}}\right| = 20\log\left|\frac{E_1}{E_{\text{in}}}\right| + 20\log_{10}|1 + A\,e^{j\theta}| \tag{7}$$

Assuming that $t_{g2} > t_{g1}$, and $\theta = -2\pi m$ where m is a positive integer, the group delay and amplitude errors simultaneously reach their upper bounds while the phase delay error given by Eq. (5) goes to zero. When $\theta = -(2n - 1)\pi$ where n is a positive integer, the group delay and amplitude errors simultaneously go to their lower bounds while the phase delay error goes to zero. However, in the case where $t_{g2} < t_{g1}$, the group delay error and carrier amplitude simultaneously reach *opposite* bounds. The expressions for upper and lower bounds on phase delay, group delay, and carrier amplitude are given in the Appendix.

Figure 2 shows plots of the upper and lower bounds of group delay in a free-space media for cases where $t_{g2} > t_{g1}$. The upper bound is obtained when the leakage and primary waves are in phase. The lower bound is obtained when the signals are out of phase. If $t_{g2} < t_{g1}$, the opposite polarity must be assigned to the $\Delta\ell$ and error-bound values of Fig. 2. For this latter case, the new upper bound will be reached when the signals are out of phase rather than in phase. (See Case 2 in the Appendix.) The signal level ripple shown on the plot is the peak-to-peak carrier signal level change as observed when θ is varied 360 deg or less. The ripple was calculated from

$$\Delta_{\text{dB}} = 20\log_{10}\frac{|E_{\text{out}}|_{\max}}{|E_{\text{out}}|_{\min}} = 20\log_{10}\left(\frac{1 + A}{1 - A}\right) \tag{8}$$

The curves shown on Fig. 2 may be useful for isolating possible sources of leakage waves on the 64-m antenna. Possible leakage can result from scattering of waves from the quadripod legs, tricone, or the dichroic plate/ellipsoid assembly support structures. Some of the differential path lengths of leakage and primary waves on the 64-m antenna can be of the order of 30 m.

III. Experimental Setup

Figure 3 shows a multipath device that was fabricated for purposes of verifying the theoretical equations presented above. Figure 4 is a block diagram of this device. To obtain the desired differential delay between path 1 and path 2, appropriate length cables can be inserted into either path 1 or path 2. The amplitude and phase of the signal in path 2 is adjusted with the variable attenuator and phase shifter, respectively. Repeatable coaxial switches were used to permit measurements of the amplitude and group delay of the signals in the individual paths.

The ranging tests were performed at the TDL in JPL Building 161. The TDL tests were performed with a 516-kHz square wave phase-modulating the uplink signal of 2113 MHz that was transmitted to an MVM'73 Radio Frequency Subsystem (RFS). After receiving the range-coded uplink, the RFS then generated a coherent 2295-MHz downlink signal that was transmitted to the Block 3 receiver through coaxial cables. The multipath device was inserted into this downlink path and therefore, adjustments made on the multipath device resulted in one-way range changes only. Measurements of absolute two-way range as well as one-way range changes were achieved with the Mu-1 ranging machine.

The initial TDL test parameters were as follows:

MVM'73 Radio Frequency Subsystem
Radio mode 022
Uplink signal level total power = −115 dBm
Block 3 Receiver
Mu-1 ranging machine
Carrier suppression = 9 dB
Integration time = 30 s

IV. Test Results

Table 1 shows a summary of the ranging test results obtained with the multipath device. Appropriate length cables were inserted into path 2 of the multipath device to create differential path lengths of 23 ns (Case A) and 93.2 ns (Case B). For each case, the signal in path 2 was adjusted to be approximately −21, −11, and −6 dB relative to the primary signal. More precise post-calibration measurements showed the leakage and primary signals to be at the relative dB levels indicated in the table. The maximum and minimum received signal levels shown in Table 1 are in reasonably good agreement with those predicted by Eqs. (A-10a) and (A-10b). The tabulated received signal levels as obtained from automatic gain control (AGC) calibrations are estimated to be accurate to ±0.2 dB.

Theoretical range change values were calculated from Eqs. (A-23a) and (A-23b). The agreement between theory and experimental range change value was typically within 1 ns. The large discrepancy of 14 ns for the last case in Part B of Table 1 could possibly be due to an error in setting the attenuator so that the relative signal level was actually −6 dB instead of the relative level of −5.5 dB on which the theoretical calculations were based. It is also possible that the discrepancy was caused by the fact that the theoretical value is valid only at a single frequency. The measured value applies to a carrier wave that is phase-modulated with a 516 kHz square wave. Therefore, for severe multipath cases it might be more appropriate to make comparisons with a theoretical value that is averaged over an effective finite bandwidth. For example, see Footnote b in Table 1.

V. Summary and Conclusions

Theoretical equations have been derived for studying the effects of multipath (or leakage) on group delay measurements. The theory was developed for group delay but is applicable to analysis of envelope delay when distortion is small. In general, very good agreement was obtained between theory and experiment.

The theory can be applied to ZDD test data to help isolate possible sources of leakage waves on the 64-m antenna. This type of analysis was done by J. R. Smith (Refs. 6, 7) for the Mariner 10 spacecraft antenna system. He showed a correlation of range change to amplitude change and isolated one of the major causes as being a multipath signal reflecting from a solar panel on the Mariner 10 spacecraft.

In this article, only one-way range error was analyzed. In a telecommunications system, the range change can be

caused by a two-way effect (uplink and downlink). The two-way range error analysis is somewhat more involved and too lengthy to include in this article. Test data on the effects of multipath on two-way range has been obtained and will be reported in a subsequent issue of this publication.

Acknowledgements

This experimental work at TDL was supported and made possible by D. L. Brunn of the Spacecraft Radio Section. M. M. Franco of the Communications Elements Research Section fabricated the multipath device.

References

1. *TRK-2-8 Module of DSN System Requirements Detailed Interface Design Document 820-13, Rev. A*, Jet Propulsion Laboratory, July 1, 1973 (JPL internal document).

2. Stelzried, C. T., Otoshi, T. Y., and Batelaan, P. D., "S/X Band Experiment: Zero Delay Device Antenna Location," in *The Deep Space Network Progress Report 42-20*, Jet Propulsion Laboratory, Pasadena, Calif., Apr. 15, 1974, pp. 64–68.

3. Schlaifer, R., "Planetary Ranging Station Delays," IOM 421-PF-TRK040, March 4, 1974 (JPL internal document).

4. Otoshi, T. Y., "Operational Support for Proposed Ranging Experiment to Resolve Range Anamolies in DSS-14 S/X System," IOM 3333-74-106, May 14, 1974 (JPL internal document).

5. Otoshi, T. Y., and Stelzried, C. T., "S/X Experiment: A New Configuration for Ground System Range Calibrations With the Zero Delay Device," in *The Deep Space Network Progress Report 42-20*, pp. 57–63, Jet Propulsion Laboratory, Pasadena, Calif., Apr. 15, 1974.

6. Smith, J. R., "Viking Ranging Investigation Team," IOM 3382-74-064, July 22, 1974 (JPL internal document).

7. Smith, J. R., "Viking Ranging Investigation Team," IOM 3382-74-076, July 30, 1974 (JPL internal document).

8. MacDoran, P. F., "A First-Principles Derivation of the Differenced Range Versus Integrated Doppler (DRVID) Charged-Particle Calibration Method," in *The Deep Space Network, Space Programs Summary 37-62, Vol. II*, pp. 28–34. Jet Propulsion Laboratory, Pasadena, Calif., Mar. 31, 1970.

9. Ramo, S., and Whinnery, J. R., "Fields and Waves in Modern Radio," John Wiley & Sons, Inc., New York, N.Y., 1953, pp. 46–48.

10. Collin, R. E., "Foundations for Microwave Engineering," pp. 132–137, McGraw-Hill Book Company, New York, N.Y., 1966.

Table 1. Results of one-way range tests with the multipath device (frequency = 2.295 GHz)

Test conditions	Phase shifter setting, deg	Approx. received signal level, dBm	Range change, ns		
			Average measured value[a]	Theoretical value	Measured minus theoretical
A. Measured delay via path 2 alone is 23.0 ns longer than path 1 alone					
1. Attenuator adjusted to make leakage signal be −21 dB relative to primary signal					
Phase shifter adjusted to obtain maximum received signal	−224.9	−89.6	1.7	1.9	− 0.2
Phase shifter adjusted to obtain minimum received signal	− 45.9	−91.2	− 2.5	− 2.3	− 0.2
2. Attenuator adjusted to make leakage signal be −10.8 dB relative to primary signal					
Phase shifter adjusted to obtain maximum received signal	−224.9	−88.1	4.8	5.1	− 0.3
Phase shifter adjusted to obtain minimum received signal	− 45.9	−93.5	−10.1	− 9.3	− 0.8
3. Attenuator adjusted to make leakage signal be −5.65 dB relative to primary signal					
Phase shifter adjusted to obtain maximum received signal	−224.9	−86.7	7.3	7.9	− 0.6
Phase shifter adjusted to obtain minimum received signal	− 45.9	−97.0	−26.4	−25.1	− 1.3
B. Measured delay via path 2 alone is 93.2 ns longer than path 1 alone					
1. Attenuator adjusted to make leakage signal be −20.7 dB relative to primary signal					
Phase shifter adjusted to obtain maximum received signal	−397.0	−89.5	7.6	7.8	− 0.2
Phase shifter adjusted to obtain minimum received signal	−218.0	−91.1	− 9.2	− 9.4	0.2
2. Attenuator adjusted to make leakage signal be −10.7 dB relative to primary signal					
Phase shifter adjusted to obtain maximum received signal	−397.0	−88.0	20.5	21.1	− 0.6
Phase shifter adjusted to obtain minimum received signal	−218.0	−93.3	−36.6	−38.7	2.1
3. Attenuator adjusted to make leakage signal be −5.5 dB relative to primary signal					
Phase shifter adjusted to obtain maximum received signal	−397.0	−86.6	31.1	32.3	− 1.2
Phase shifter adjusted to obtain minimum received signal	−218.0	−97.0	−91.2	−105.2[b]	14.0

[a]Number of 30-sec integration data points used to obtain average value was typically 20. The calculated standard error associated with the average was typically ± 0.2 ns.

[b]The average theoretical range change over the frequency range of 2295.0 ± 0.5 MHz is −96.4 ns.

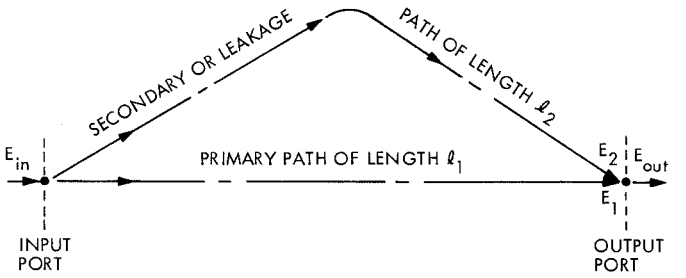

Fig. 1. Geometry for multipath analysis

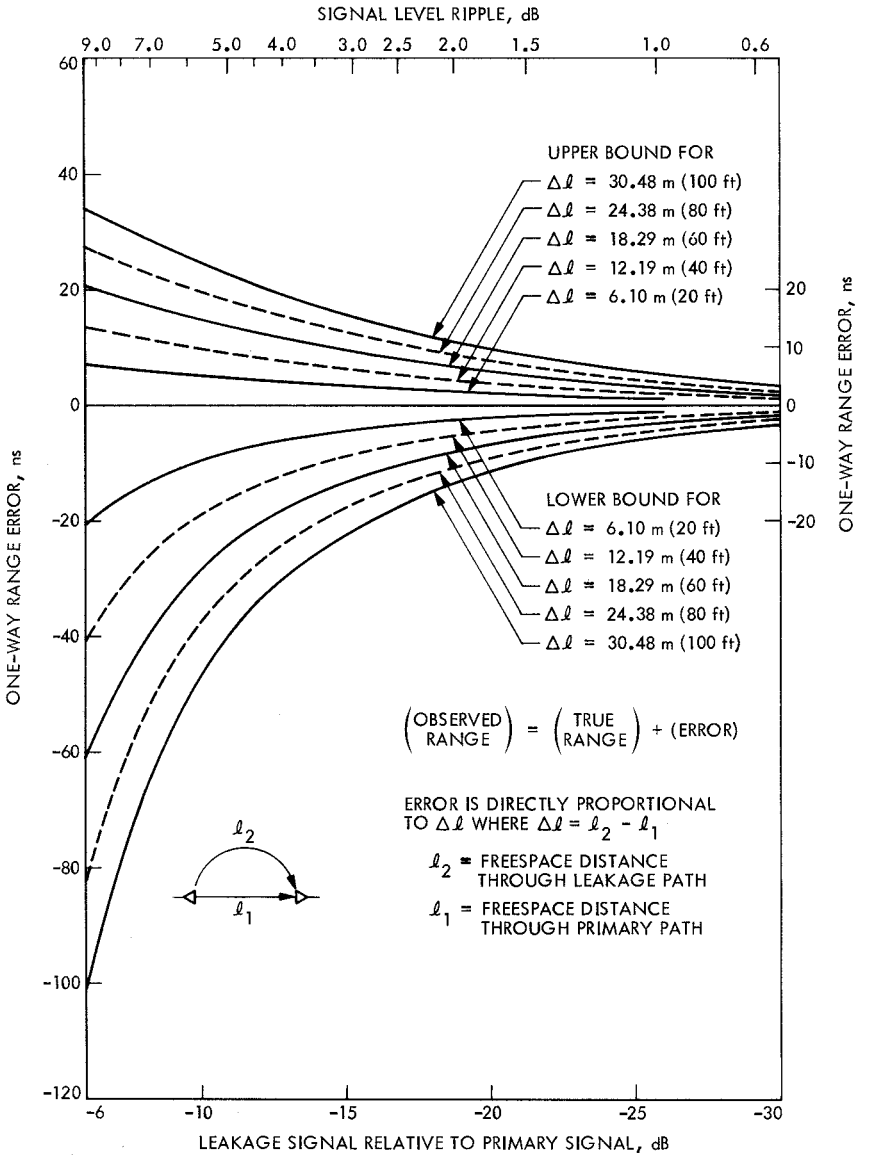

Fig. 2. Limits of one-way range error due to multipath in a free-space media

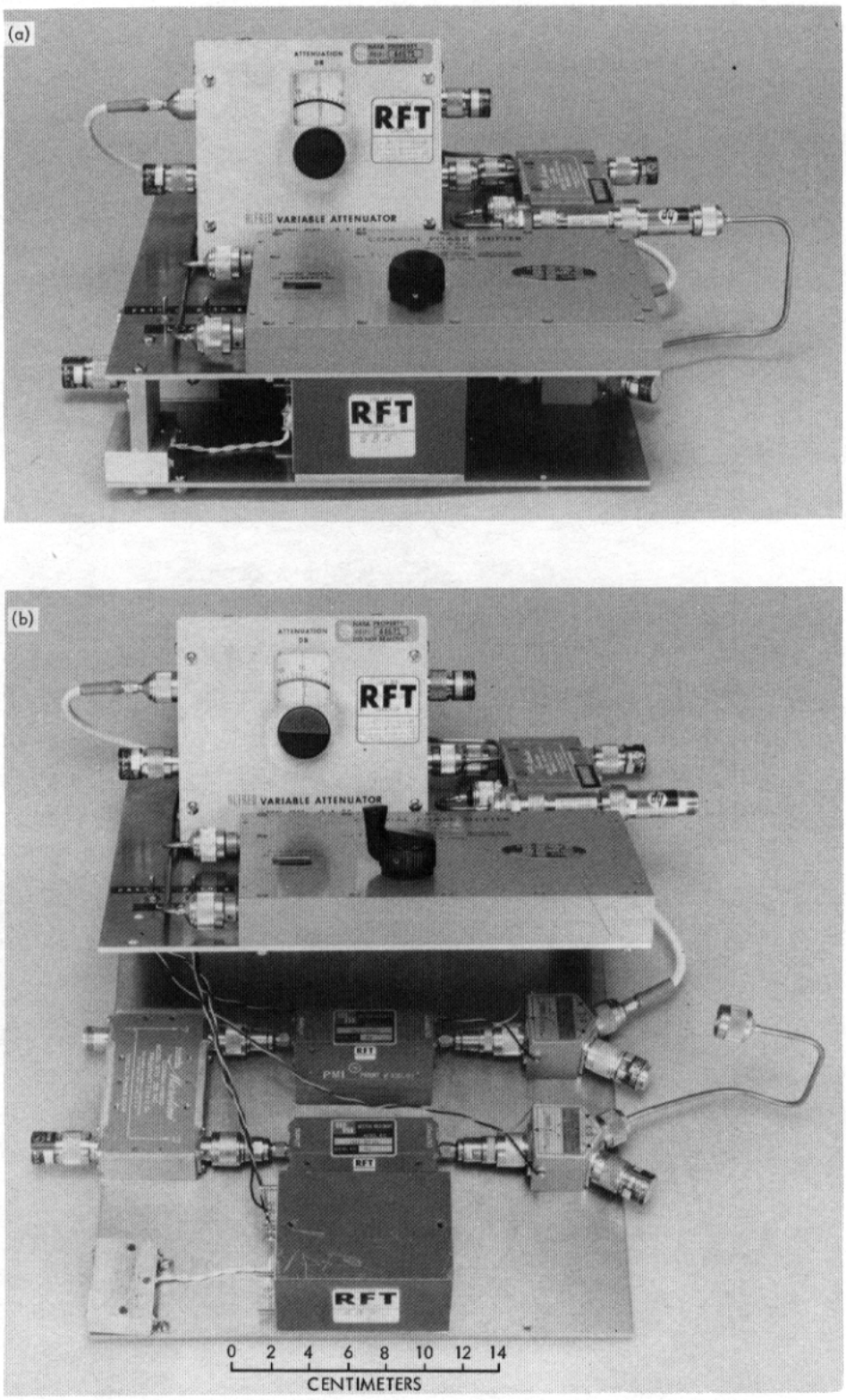

Fig. 3. Multipath device for experimental verification of theoretical derivations: (a) completely assembled, (b) partially disassembled

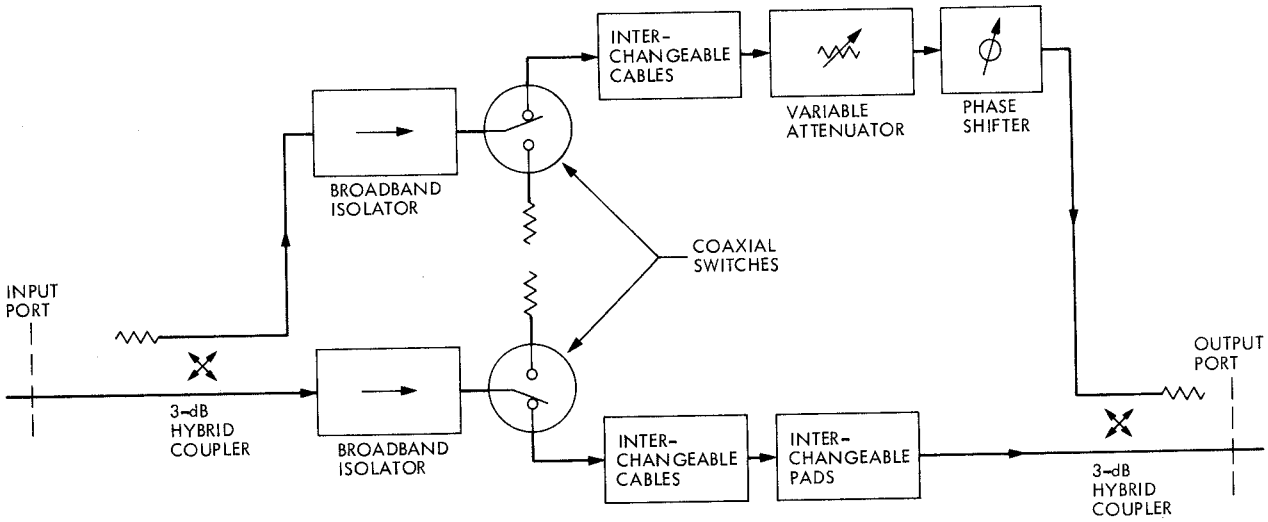

Fig. 4. Multipath device block diagram

Appendix

Derivation of Equations for Phase and Group Delay Errors Caused by Multipath

Figure 1 shows the basic multipath configuration under study where two waves combine after traveling through two separate paths. This basic case can be generalized to include more waves and more paths, but it is sufficient to consider the basic case to show the effect of interference on group delay. Let the wave at the input port be expressed as

$$E_{in} = |E_{in}| \exp(j\phi_0) \tag{A-1}$$

and the wave at the output port be the phasor sum of the primary path wave E_1 and the secondary path wave E_2 so that

$$\begin{aligned} E_{out} &= E_1 + E_2 \\ &= |E_1| \exp(j\phi_1) + |E_2| \exp(j\phi_2) \end{aligned} \tag{A-2}$$

Then from Eqs. (A-1) and (A-2)

$$\frac{E_{out}}{E_{in}} = \left|\frac{E_1}{E_{in}}\right| \exp j(\phi_1 - \phi_0) + \left|\frac{E_2}{E_{in}}\right| \exp[j(\phi_2 - \phi_0)] \tag{A-3}$$

Let

$$\phi_1 - \phi_0 = -\beta_1 \ell_1 \tag{A-4}$$

$$\phi_2 - \phi_0 = -\beta_2 \ell_2 \tag{A-5}$$

where

ℓ_1 = physical length of path 1, m

ℓ_2 = physical length of path 2, m

β_1, β_2 = phase constants, respectively, of paths 1 and 2, rad/m

Substitution of Eqs. (A-4) and (A-5) into Eq. (A-3) gives

$$\frac{E_{out}}{E_{in}} = \left|\frac{E_1}{E_{in}}\right| \exp(-j\beta_1\ell_1)\left[1 + \left|\frac{E_2}{E_1}\right| \exp[-j(\beta_2\ell_2 - \beta_1\ell_1)]\right] \tag{A-6}$$

The ratio $|E_2/E_1|$ is a parameter that is generally of interest so that it is convenient to let

$$A = \left|\frac{E_2}{E_1}\right| \tag{A-7}$$

Furthermore, let

$$\theta = -(\beta_2\ell_2 - \beta_1\ell_1) \tag{A-8}$$

and

$$F = 1 + A e^{j\theta} \tag{A-9}$$

so that substitution into Eq. (A-6) gives the output signal magnitude ratio of

$$\left|\frac{E_{out}}{E_{in}}\right| = \left|\frac{E_1}{E_{in}}\right| |1 + A e^{j\theta}| \tag{A-10}$$

and relative phase of

$$\arg\left(\frac{E_{out}}{E_{in}}\right) = -\beta_1\ell_1 + \arg F \tag{A-11}$$

where

$$\arg F = \tan^{-1}\left[\frac{A \sin\theta}{1 + A\cos\theta}\right] \tag{A-12}$$

From substitution of Eq. (A-11) into the definition of phase delay (Refs. 9, 10) given as

$$t_p = \frac{-1}{\omega}\left[\arg\left(\frac{E_{out}}{E_{in}}\right)\right] \tag{A-13}$$

we obtain

$$t_p = t_{p1} + \epsilon_p \tag{A-14}$$

where

$$t_{p1} = \frac{\beta_1\ell_1}{\omega} \tag{A-15}$$

$$\epsilon_p = -\frac{1}{\omega}\tan^{-1}\left[\frac{A\sin\theta}{1 + A\cos\theta}\right] \tag{A-16}$$

From setting the differential of ϵ_p with respect to ℓ_2 equal to zero, one finds that ϵ_p becomes maximum when $\theta = \pm\cos^{-1}(-A)$ so that the upper and lower bounds of phase delay error are

$$(\epsilon_p)_U = +\frac{1}{\omega}\tan^{-1}\left(\frac{A}{\sqrt{1 - A^2}}\right) \tag{A-17}$$

$$(\epsilon_p)_L = -\frac{1}{\omega}\tan^{-1}\left(\frac{A}{\sqrt{1-A^2}}\right) \qquad \text{(A-18)}$$

The worst possible case occurs when $A \rightarrow 1$ and the error bounds become $\pm 1/(4f)$. For example, at 2.0 GHz the worst-case phase delay error that can be caused by multipath is ± 0.125 ns.

The definition of group delay (Refs. 9, 10) is

$$t_g = -\frac{d}{d\omega}\left[\arg\left(\frac{E_{\text{out}}}{E_{\text{in}}}\right)\right] \qquad \text{(A-19)}$$

From substitution of Eq. (A-11) into Eq. (A-19), we obtain

$$t_g = t_{g1} + \epsilon_g \qquad \text{(A-20)}$$

where

$$t_{g1} = \frac{d\beta_1}{d\omega}\ell_1 \qquad \text{(A-21)}$$

$$\epsilon_g = -\frac{d}{d\omega}\arg F \qquad \text{(A-22)}$$

where arg F was given by Eq. (A-12). Note that t_{g1} is the group delay that would be obtained in the absence of multipath and ϵ_g is the group delay error or deviation from t_{g1}.

Performing the operation of Eq. (A-22) and assuming that over the frequency interval of interest

$$\frac{\partial A}{\partial \omega} = 0$$

we obtain

$$\epsilon_g = A(t_{g2} - t_{g1})\left(\frac{A + \cos\theta}{1 + 2A\cos\theta + A^2}\right) \qquad \text{(A-23)}$$

where

$$t_{g2} = \left(\frac{d\beta_2}{d\omega}\right)\ell_2$$

$$t_{g1} = \left(\frac{d\beta_1}{d\omega}\right)\ell_1$$

Note that t_{g1} is the delay through path 1 only in the absence of the multipath signal, while t_{g2} is the delay through path 2 only.

Performing a differentiation[1] of Eq. (A-23) with respect to ℓ_2 and setting the results equal to zero leads to the solutions of the values of θ which give upper and lower bounds of ϵ_g for two different cases. These are given as follows.

Case 1 Upper Bound

Assume $t_{g2} > t_{g1}$ and $\theta = -2\pi m$ where θ was given by Eq. (A-8) and m is a positive integer. In practice, m will usually be an integer greater than 10.

For these conditions, the leakage and primary waves are in phase and the group delay as given by Eq. (A-23) reaches an upper bound of

$$(\epsilon_g)_{U1} = (t_{g2} - t_{g1})\left(\frac{A}{1+A}\right) \qquad \text{(A-23a)}$$

At the same time, note from Eqs. (A-10) and (A-16) that the output signal magnitude ratio and phase delay error become

$$\left|\frac{E_{\text{out}}}{E_{\text{in}}}\right| = \left|\frac{E_1}{E_{\text{in}}}\right|(1 + A) \qquad \text{(A-10a)}$$

$$\epsilon_p = 0 \qquad \text{(A-16a)}$$

It is interesting to note that both the group delay and magnitude of the output signal reach an upper bound simultaneously while the phase delay error goes to zero.

Case 1 Lower Bound

Assume $t_{g2} > t_{g1}$ and $\theta = -(2n-1)\pi$ where θ is defined by Eq. (A-8) and n is a positive integer. In practice, n will usually be an integer greater than 10.

For these conditions, the leakage and primary waves are out of phase and the group delay error as given by Eq. (A-23) reaches a lower bound of

$$(\epsilon_g)_{L1} = -(t_{g2} - t_{g1})\left(\frac{A}{1-A}\right) \qquad \text{(A-23b)}$$

and the output signal magnitude ratio as given by Eq. (A-10) also reaches a lower bound of

$$\left|\frac{E_{\text{out}}}{E_{\text{in}}}\right| = \left|\frac{E_1}{E_{\text{in}}}\right|(1 - A) \qquad \text{(A-10b)}$$

[1]In the differentiation, it is assumed that the radian frequency ω is sufficiently large so that large changes of θ occur with small changes of ℓ_2. Then in the interval over which θ undergoes a 360-deg change, $\partial t_{g2}/\partial \ell_2 \simeq 0$. For those special cases where these assumptions are not valid or where more accuracy is required, one can obtain the exact bounds from incrementing ℓ_2 and performing numerical computations of Eq. (A-23).

while the phase delay error as given by Eq. (A-16) is zero.

Case 2 Upper Bound

Assume $t_{g1} > t_{g2}$ and $\theta = (2n - 1)\pi$ where θ is defined by Eq. (A-8) and n is a positive integer. In practice, n will usually be an integer greater than 10.

Under these conditions, the leakage and primary waves are out of phase, but in contrast to Case 1, the group delay error reaches an upper bound of

$$(\epsilon_g)_{U2} = (t_{g1} - t_{g2})\left(\frac{A}{1 - A}\right) \qquad \text{(A-23c)}$$

when the output signal magnitude ratio reaches a *lower* bound of

$$\left|\frac{E_{out}}{E_{in}}\right| = \left|\frac{E_1}{E_{in}}\right|(1 - A) \qquad \text{(A-10c)}$$

and the phase delay error as calculated from Eq. (A-16) is zero.

Case 2 Lower Bound

Assume $t_{g1} > t_{g2}$ and $\theta = 2\pi m$ where θ is given by Eq. (A-8) and m is a positive integer. In practice, m will usually be an integer greater than 10.

Under these conditions the leakage and primary waves are in phase, but the group delay error goes to its lower bound of

$$(\epsilon_g)_{L2} = -(t_{g1} - t_{g2})\left(\frac{A}{1 + A}\right) \qquad \text{(A-23d)}$$

Simultaneously, the output signal magnitude ratio reaches an upper bound of

$$\left|\frac{E_{out}}{E_{in}}\right| = \left|\frac{E_1}{E_{in}}\right|(1 + A) \qquad \text{(A-10d)}$$

and the phase delay error goes to zero.

Differenced Range Versus Integrated Doppler

A parameter which is of primary importance to radio science experiments with a spacecraft is differenced range versus integrated doppler which can be expressed as (Ref. 8)

$$\text{DRVID} = t_g - t_p \qquad \text{(A-24)}$$

Then substitutions of Eqs. (A-14) to (A-16) and Eqs. (A-20) to (A-23) give

$$\text{DRVID} = \left(\frac{d\beta_1}{d\omega} - \frac{\beta_1}{\omega}\right)\ell_1 + A(t_{g2} - t_{g1})\left(\frac{A + \cos\theta}{1 + 2A\cos\theta + A^2}\right) + \frac{1}{\omega}\tan^{-1}\left[\frac{A\sin\theta}{1 + A\cos\theta}\right] \qquad \text{(A-25)}$$

Note that in a dispersionless system

$$\frac{d\beta_1}{d\omega} = \frac{\beta_1}{\omega}$$

and in the absence of multipath, $A = 0$, so that

$$\text{DRVID} = 0$$